DUPLICATE ALSO

Short-range Forecasting Research

204

Short Range Forecasting Division

Scientific Paper No.4

DIAGNOSIS OF VISIBILITY IN THE UK MET OFFICE MESOSCALE MODEL AND THE USE OF A VISIBILITY ANALYSIS TO CONSTRAIN INITIAL CONDITIONS

by

S P Ballard , B J Wright and B W Golding

April 1992

Meteorological Office
London Road
Bracknell
Berkshire
RG12 2SZ
United Kingdom

ORGS UKMO S

National Meteorological Library
FitzRoy Road, Exeter, Devon. EX1 3PB

Short-Range Forecasting Research Division

Scientific Paper No 4

DIAGNOSIS OF VISIBILITY IN THE UK MET OFFICE MESOSCALE MODEL AND THE USE OF A VISIBILITY ANALYSIS TO CONSTRAIN INITIAL CONDITIONS

by

S P Ballard , B J Wright and B W Golding

April 1992

Short-Range Forecasting Research Division
Meteorological Office
London Road
Bracknell
Berkshire
RG12 2SZ
ENGLAND

N.B. This paper has not been published. Permission to quote from it must be obtained from the above Met Office division.

Diagnosis of visibility in the UK Met Office Mesoscale Model

and the use of a visibility analysis to constrain initial conditions

S P Ballard , B J Wright and B W Golding*
Mesoscale Forecast and Analysis Group
Short Range Forecasting Research Division
Meteorological Office, London Rd , Bracknell, UK
Fax number - 0344-854412
E-mail number A.Lorenc/OMNET for attn S P Ballard

* Presently at BMRC, Melbourne, Australia

Prepared for the MIT LL meeting on ceiling and visibility
at MIT campus, 10th April 1992.

1. Introduction

Various papers have addressed the problem of forecasting fog, using models to predict or simulate the formation, evolution and dispersal of fog or described observational studies (Tremant 1989, Brown and Roach 1976, Brown 1980, Bott et al 1990, Cotton and Anthes 1989, Duynkerke 1991, Musson-Genon 1987, Oliver at al 1978, Tjernstrom 1987, Roach et al 1976, Turton and Brown 1987, Zdunkowski and Barr 1972, Vehil at al 1989, Pilie at al 1979, Findlater et al 1989). The ability of the UK Met Office mesoscale model to predict sea fog and its sensitivity to initial conditions was described in Ballard et al 1991 and the general performance of the model in predicting fog was described briefly in Golding 1990 and Ballard and Golding 1990. The interactive mesoscale initialisation (IMI) was described in Wright and Golding 1990. This paper describes the current system used to diagnose visibility from mesoscale model forecast fields and the use of a visibilty analysis to initialise boundary layer cloud , humidity and aerosol or cloud condensation nuclei concentration fields. The scheme has been implemented in the programs used to process output fields, provide chart/graphical output and to perform the automatic or interactive mesoscale initialisation.

2. Diagnosis of visibility from model output fields

The mesoscale model currently has levels near the surface at heights of 1.25, 2.5, 5, 10, 20 , 40, 70, 115m respectively. The previous version of the model had levels at 10 and 110m only. At these levels values of cloud condensate (water or ice) mixing ratio (CWMR kg/kg) and relative humidity (RH fraction, calculated from prognostic variables humidity mixing ratio kg/kg, potential temperature and pressure) are predicted. An additional single level variable representing boundary layer aerosols or cloud condensation nuclei concentrations (CCN cm^{-3}) is also predicted from advection of initialised values using the horizontal wind at the level nearest to 1km.

On output a value of visibility can be diagnosed, this is usually calculated at the level nearest to 5m above ground. The visibility is calculated using the relationship

$$vis = \frac{0.000978}{\{\log_{10}(CN)+0.25\}\times CW^{2/3}}$$

where CN = max (20, CCN) in units cm^{-3}

and CW = max (CWMR, CW')

$$CW' = \frac{-0.2618 \times 10^{-9} \times CCN}{\ln(RH)}$$

$0.01 < RH < 0.999$

Note the lower limit on the value of CCN is only used in the calculation of the visibility and not in the calculation of CW'. This may cause problems if the CCN field is not defined, as in its use for calculation of visibility from the unified model. In the mesoscale model if values of CCN are not derived from a visibility analysis values of 200 cm^{-3} for land, 50 cm^{-3} for sea and 500 cm^{-3} for urban sites are set. The model boundary conditions use values of 200 cm^{-3} for land and 50 cm^{-3} for sea.

3. Source of visibility relationship

The observation and definition of visibility through the atmosphere is related to the contrast between the luminance of an object, B, and the background, B'. The contrast, C, is defined as

$$C = (B - B')/B'$$

Koschmeider 1924, summarised in Middleton 1952, provided a theory of visual range in the horizontal. He derived the relationship between the luminance of a black object at distance r, B_b and the horizon sky, B_h as

$$B_b = B_h(1-e^{-\beta r})$$

where β is the extinction coefficient of the atmospheric path.

This gives

$$C_R = C_0 e^{-\beta R}$$

where C_0 is the contrast if both the object and the sky are seen at close range and C_R is the contrast when both are at distance R, assuming that the luminance of the background, the horizon sky, does not change as the object is approached.

The visual range is defined as the distance at which the contrast reduces to a given liminal contrast. Koschmeider assumed a liminal contrast of 0.02 for the visual range of objects seen against the horizon sky.

Therefore the equation relating the visibility, or visual range, to the extinction coefficient is given by:

$$vis = - \frac{\ln \varepsilon}{\beta} \qquad (3.1)$$

where β is the extinction coefficient in km^{-1} and ε is the threshold of contrast and is normally assumed equal to Koschmeider's value of 0.02 so that

$$vis = \frac{3.912023}{\beta} \qquad (3.2)$$

The value of 0.02 for the threshold of contrast is used in the mesoscale model scheme but it should be noted that WMO recommend a value of 0.05 so that

$$vis = \frac{3.0}{\beta} \qquad (3.2a)$$

If the dropsize distribution is known β can be readily calculated from

$$\beta = \pi \sum_{i=1}^{N} Q_{ext}\ n_i\ r_i^2 \qquad (3.3)$$

where Q_{ext} is the normalized extinction cross-section.

However the model does not predict the dropsize distribution, only the liquid water content and an empirical relationship is required to relate CWMR to β. Various relationships have been proposed such as Eldridge 1966, 1971, Pinnick et al 1978, Tomasi and Tamieri 1976 and Kunkel 1983 . Kunkel 1983 summarised the results of the earlier papers which all gave a two-thirds relationship (β proportional to $W^{2/3}$, where W is liquid water content in g m^{-3}) but derived a more linear relationship based on measurements in 11 fogs at Otis National Guard Base, Massachusetts during 1980-1981. He states that this is due to the earlier observations having smaller droplets in the lighter fogs than the droplets in the denser fogs. The results show that the extinction coefficient is affected by the purity of the fog - a polluted fog yielding higher extinction coefficient, or

lower visibilities, for a given liquid water content. This is due to a decrease in terminal velocity, reducing fallout of water, and an increase in the number of particles. Therefore in the prediction of visibility it is important to define the concentration of pollutants as well as liquid water.

Kunkel 1983 derived formulae for all the 11 Otis fogs as well as polluted and clean fogs separately as

$$\begin{aligned} \beta &= 144.7 \times W^{0.88} && \text{mean for all Otis fogs} \\ \beta &= 99 \times W^{0.92} && \text{for clean air} \\ \beta &= 162 \times W^{0.84} && \text{for dirty air} \end{aligned} \qquad (3.4)$$

However, due to reservations about the shape of the mean curve, the mesoscale model visibility calculation is based on the earlier results of Tomasi and Tampieri 1976

$$\begin{aligned} \beta &= 65 \times W^{2/3} && \text{for clean air} \\ \beta &= 115 \times W^{2/3} && \text{for dirty air} \end{aligned} \qquad (3.5)$$

to parameterise β as a function of CCN conc. (cm^{-3}) as well as W ($g\ m^{-3}$) as follows:

$$\beta = (40 \times \log_{10}(CCN) + 10) \times W^{2/3} \qquad (3.6)$$

Equations 3.2 and 3.6 can be combined to give:

$$vis = \frac{0.0978}{\{\log_{10}(CCN) + 0.25\} \times W^{2/3}} \qquad (3.7)$$

using CWMR in kg/kg rather than W and assuming the density of air to be 1 $kg\ m^{-3}$ near the surface gives

$$vis = \frac{0.000978}{\{\log_{10}(CCN) + 0.25\} \times CWMR^{2/3}} \qquad (3.8)$$

as a diagnostic relationship for visibility in km given CCN in cm^{-3} and CWMR in kg/kg.

The use of the more linear relationship devised by Kunkel 1983 would result in lower extinctions in light fogs and higher extinctions in dense fogs for a given liquid water content and CCN value than given by equation 3.8. It would be interesting to study the verifcation figures for the mesoscale model to see whether it could benefit from a revised formula. There is certainly a tendency to forecast visibilities that are too low when mist, with visibilities above the aviation fog threshold of 1km, is observed.

Equation 3.8 only gives diagnosed visibilities when cloud liquid water is present. In order to cover the whole range of visibilities the work of Hanel 1987 has been adapted to give a relationship in terms of CCN and relative humidity.

4. Derivation of relationship between relative humidity, CCN and visibility

When there is no gridscale cloud condensate present, ie the predicted CWMR is zero, reduced visibilities are assumed to be due to the presence of 'subgridscale' cloud condensate that has formed around aerosols or cloud condensation nuclei. The total amount of 'subgridscale' cloud water present will depend on the ambient relative humidity and the concentration of nuclei . A particle or droplet grows if the relative humidity RH of the ambient air is larger than the relative humidity of the air at the particle or droplet surface, shrinks if it is smaller and is in equilibrium if they are equal. Hanel 1987 gives the equilibrium relative humidity at the particles surface as

$$RH = \exp\left[\frac{A^0}{r} - \frac{B^0}{(r/r_d)^3-1}\right] \qquad (4.1)$$

take values of $A^0 = 1.2\times10^{-9}$m = curvature parameter
$B^0 = 0.5$ = activation parameter
and r_d = volume equivalent radius of a dry particle
ie aerosol or cloud condensation nucleus

Assuming that the first term can be neglected.

$$RH = \exp\left[\frac{-B^0}{(r/r_d)^3 - 1}\right] \qquad (4.2)$$

This can be rearranged to give an expression for the radius of the water droplets.

$$r^3 = \frac{-B^0}{\ln(RH)} \times r_d^3 + r_d^3 \qquad (4.3)$$

The volume of water in the droplet ,excluding dry aerosol, is given by

$$vol = \frac{4}{3}\times\pi\ (r^3-r_d^3)$$

substituting for the radius from equation gives:

$$vol = \frac{-4\pi r_d^3\times B^0}{3\times\ln(RH)} \qquad (4.4)$$

Multiplying by the number of CCN/m^3 and the density of water gives the total mass of liquid water per m^3.

$$mass/m^3 = \frac{-4\pi r_d^3\times B^0\times\rho_w\times CCN\times10^6}{3\times\ln(RH)} \qquad (4.5)$$

The 'subgridscale' CWMR, CW' is obtained by simply dividing by the density of air.

$$CW' = \frac{-4\pi r_d^3\times B^0\times\rho_w\times CCN\times10^6}{3\times\ln(RH)\times\rho_a} \qquad (4.6)$$

Taking the values: $\rho_a = 1$ kg/m^3
$\rho_w = 1000$ kg/m^3
$r_d = 0.5$ µm
$B^0 = 0.5$

gives the expression:

$$CW' = \frac{-\pi \times CCN}{12 \times 10^9 \times \ln(RH)} \qquad (4.7)$$

which is used in the formula for visibility in the absence of significant amounts of gridscale cloud water or ice.

5. Visibility Analysis and its use in initialisation of CCN, CWMR and RH

An analysis of surface visibility reports is carried out as part of the mesoscale model initialisation. At 00Z and 06Z this is performed interactively but at other times, 3 hourly throughout the day and night, it is run automatically.

The visibility diagnosed from a 3 hour mesoscale forecast is used as the first guess for the analysis. When the bottom level was at 10m the diagnosed visibility at that level was used, with higher vertical resolution the level at or nearest 5m is used.

A recursive filter analysis scheme is used (Purser and McQuigg 1982, Hayden and Purser 1986, Hayden and Purser 1988), see Appendix B. The log of visibility is analysed rather than the variable itself.

In interactive mode the analysis is displayed to the forecaster in a symbol representation (see table 1), with observations as numbers.

Visibility	Symbol	Description
0 - 200 m	F	Public service fog
200 m - 1 km	F	Aviation fog
1 - 5 km	-	Mist
> 5 km	<blank>	Good visibility

Table 1 Symbols for visibility analysis.

The analysed visibility is then used as part of the initialisation of the boundary layer humidity and cloud condensation nuclei concentration.

The cloud cover, cloud water mixing ratio (CWMR) and relative humidity below 20 m are initialised using the analysed visibility .

The level nearest to 5 m AGL is selected for the initial calculations. The cloud condensation nuclei concentration (CCN conc.) is limited to be greater than 20 cm^{-3}. If no CCN conc. field is present in the dataset, then one will be created with values of 50 and 200 cm^{-3} for sea and land areas respectively. A CWMR is then deduced from the visibility and CCN conc. using the equation :

$$CWMR' = \left[\frac{0.000938}{vis \times \{\log_{10}(CCN)+0.25\}}\right]^{1.5} \qquad (5.1)$$

Note the use of 0.000938 is an error and 0.000978 should be used.

The value of CWMR' is limited to 2 g/kg. The relative humidity is computed from the analysed dewpoint and the pressure and temperature (which have been adjusted based on analysed fields). Upper and lower limits are calculated for the relative humidity from the value of CWMR', assuming

limits of 20 and 500 cm^{-3} on the CCN conc. using the equation :

$$RH^{low} = \exp\left[\frac{-500\times0.2618\times10^{-9}}{CWMR'}\right] \quad (5.2)$$

$$RH^{high} = \exp\left[\frac{-20\times0.2618\times10^{-9}}{CWMR'}\right] \quad (5.3)$$

For visibilities less than 1.5 km or relative humidities greater than 0.99, the CWMR is set equal to CWMR', the cloud cover is set to 8 oktas and the relative humidity is set to 1. No adjustment is made to CCN conc. as the CWMR is the important factor determining visibility when gridscale cloud condensate is present.

For higher visibilities and lower humidities, the CWMR and the cloud cover are set to 0, the relative humidity is left unadjusted, but the CCN conc. is recalculated to be consistent with the value of CWMR' which is now assumed to be a 'subgridscale' cloud condensate using the results of section 4.

$$CCN = \frac{-CWMR'\times\ln(RH)}{0.2618\times10^{-9}} \quad (5.4)$$

The CCN conc. is then smoothed, using upstream weighting of e^{-1}, in two complete sweeps.

For other levels below 20 m, the relative humidity is recalculated assuming the same humidity mixing ratio, but using the pressure and temperature at the new level. The relative humidity is then limited using the limits calculated originally. Cloud cover, CWMR and relative humidity are set as for the level nearest to 5 m, but CCN conc. is not modified, as it is only carried at a single level, which represents the boundary layer.

6. Derivation of formulae used in initialisation of CWMR, CCN and RH using a visibility analysis.

Within the IMI analysed values of visiblity and relative humidity are obtained and a first guess value of CCN conc. is available. From these quantities we wish to calculate an improved value of CCN conc. and a value of CWMR. So we need equations relating visibility, relative humidity, CWMR and CCN conc..

The formula used to diagnose visibility from forecast fields is:

$$vis = \frac{0.000978}{\{\log_{10}(CCN)+0.25\}\times CWMR^{\frac{2}{3}}}$$

This equation relating visibility to CWMR can rearranged into a form that can be used to estimate the CWMR from the analysed visibility and the first guess CCN conc..

$$CWMR = \left[\frac{0.000978}{\{\log_{10}(CCN)+0.25\}\times vis}\right]^{1.5} \quad (6.1)$$

The expression for CWMR in terms of relative humidity and CCN from section 4

$$CWMR = \frac{-\pi\times CCN}{12\times10^{9}\times\ln(RH)} \quad (6.2)$$

can be rearranged to give an equation that can be used to obtain an

improved estimate of the CCN conc..

$$CCN = 3.82\times10^{9}\times CWMR\times \ln(RH) \qquad (6.3)$$

Or to obtain an estimate of relative humidity.

$$RH = \exp\left[\frac{-0.2618\times10^{-9}\times CCN}{CWMR}\right] \qquad (6.4)$$

Equation 6.4 is used to constrain the analysed relative humidity using the calculated CWMR , and CCN conc. values of 20 and 500 cm^{-3} as in equations 5.2 and 5.3.

7.Implimentation of diagnosis of visibility in the new UK Met Office Unified Model

A new 'unified' model has been introduced in the UK Met Office to produce the global (approx 100km, 20 levels) 5 day forecasts and the limited area (approx 50km, 20 levels) 2 day forecasts. Its performance at high resolution (16.8km and 31 levels) is currently being assessed to see whether it could be used operationally as a replacement for the current mesoscale model. This would reduce maintenance costs and development of the model for mesoscale forecasting would then potentially feed back directly to the global and even climate modelling. The unified model currently has a bottom eta (hybrid sigma at low levels to pressure at upper levels) level at about 25m and values of fields within the surface layer (eg wind at 10m and screen temperature at 1.5m) are diagnosed using Monin-Obukhov similarity theory including the stability of the surface layer. Currently only 10m wind and screen temperature are available as output from the model from within the surface layer. Therefore the lowest level at which visibility can be diagnosed is at 25m. There is no variable equivalent to CCN at present in the unified model. Code has been written to calculate visibility at 25m using output fields of cloud water, cloud ice, and specific humidity (relative humidity is not available so is calculated using the saturation humidity mixing ratio at the 25m temperature). The same formula is used as for the current mesoscale model, ie the formula given in section 2, but a value of 200 cm^{-3} is assumed for the CCN concentration. The next version of the unified model allows the output of values of cloud water, cloud ice and specific humidity from within the surface layer so in future the visibility can be calculated at screen height (1.5m) or with extensions to the code at other levels such as 5m. It is possible that extra near surface layers are required for accurate fog prediction and this may be tested at a later date. Resource limitations have meant that it has not been possible to ascertain whether there has been any benefit from reducing the bottom level of the current mesoscale model and resolving the near surface vertical structure.

8. Performance of mesoscale model visibility prediction

The model generally overpredicts fog, ie visibility less than 1km. One reason for this is that the model currently underpredicts stratocumulus due to initialisation problems so there are too many clear, radiatively cooling, nights. Also fog is often predicted at 5m above ground when only mist or shallow fog is reported with visibilities greater than 1km. Predicted locations of fog can show skill but forecasters would prefer greater accuracy . Currently the model is not retaining fog throughout the

day. Winter 1991/92 in the UK has seen many occassions of persistant fog lasting for days on end, much of this was also freezing fog. The model is run twice daily 0 UTC for 18 hours 6 UTC for 30 hours. Forecasts initialised at 0 UTC generally tend to lose the persistant fog after sunrise - 9 UTC to 10 UTC in winter - however some forecasts initialised at 6 UTC have maintained some fog, but not enough, throughout the day. It is possible that the fog is not being initialised deep enough or there may be problems with the radiation scheme in the model.

An initial pre-trial of the high resolution version of the unified model has just been run. This included a freezing fog case where fog had been present for a few days and caused many flight cancellations at Heathrow. The fog remained throughout the day but dispersed slightly overnight. The operational forecast initialised at 0 UTC 14/12/91 with fog lost it during the late morning. The operational forecast initialised at 6 UTC retained some fog throughout the day but increased the area after sunset to give widespread fog throughout the night rather than decreasing the coverage overnight. A forecast using the current mesoscale model but running from interpolated regional model (50km resolution, 20levels) fields retained no fog during the day and overpredicted even more the following night. Forecasts from the high resolution version of the unified model (16.8km, 31 levels) with and without data assimilation (no cloud or visibility analysis, just radiosondes, pmsl, 10m winds over the sea) had only small areas of fog in south Wales during the first morning but also forecast no fog during the day and formed fog later in the second night, not quite so much overprediction but the location was wrong - ie in west rather than east of England. The regional model itself again had no fog (visibility less than 1km) during the first day and vastly overpredicted fog the following night (9 UTC 15/12/91 60% of verification stations as opposed to 16.1 % observed, 27.6% from the operational mesoscale model and 23.4 % from the high resolution model with data assimilation). These results show the benefit of improved resolution and an initialisation scheme for fog. (note visibility was at 25m in unified model as opposed to 5m in the mesoscale model).

Figure 1 shows the predicted present weather, ie visibilities at 5m or precipitation, at 6 hourly intervals from a sequence of 4 operational forecasts covering the period 0 UTC 14/12/91 to 18 UTC 15/12/91. These can be compared with the observed visibilities shown in figure 2. There are obviously large differences between forecasts of different periods verifying at the same time. The reason for the erroneous large areas of widespread fog in the initial conditions at 0 UTC 15/12/91 and 6 UTC 15/12/91 has not yet been investigated. In the present weather display the visibility is not shown if there is precipitation present.

Figure 2 shows forecast visibilities from the high resolution version of the unified model with data assimilation data time 6 UTC 14/12/91 (at 25m) and from the mesoscale model forecast from interpolated regional model analysis for 6 UTC 14/12/91 (at 5m) as well as the observed visibilities. These can be compared with the predictions from the operational forecast in figure 1 however the first figure does not distinguish between visibilities below 200m and between 200m and 1km.

9. Future Work

Far more in depth studies are required of the ability of mesoscale models to give accurate predictions of the presence of fog and the actual visibility. Only very limited studies of the performance of the current model have been undertaken. The high level of prognostic skill expected by the forecasters may be unrealistic considering the limited resolution and data sources available to the current model.

Forecasts of the presence of fog are obviously sensitive to the accuracy of the initial conditions and surface characteristics as well as the prognostic skill of the model for cloud cover, low level humidity, temperatures and surface fluxes. At 15km resolution the mesoscale model is not resolving the local valleys and drainage flows or surface moisture sources such as rivers and lakes and this will obviously limit the prognostic skill for radiation fog. Sensitivity studies to horizontal and vertical resolution, physical parametrizations and surface characteristics as well as initial conditions are required.

The forecast skill for visibility is also dependent on the accuracy of the diagnostic formulae. Various areas where slightly different formulae could be used have been pointed out in the text such as the parametrization of β with respect to cloud condensate and cloud condensation nuclei concentration. This paramterization and the CCN scheme itself is greatly simplified . The latter may need to be extended to predict a full 3D distribution of aerosol, to include sources and sinks , and to become interactive rather than just diagnostic, ie including the CCN concentration in the generation of cloud condensate and in radiation schemes.

References

Ballard, S.P. and Golding, B.W.
1990 The UK Met Office Mesoscale model - operational experiences, proceedings of HIRLAM workshop on mesoscale modelling, Copenhagen, Denmark 3-5 September 1990

Ballard, S.P., Golding, B.W. and Smith, R.N.B.,
1991 Mesoscale model experimental forecasts of the Haar of north east Scotland. *Mon Wea Rev* 119 2107-2123.

Bott, A., Sievers, U. and Zdunkowski, W.
1990 A radiation fog model with a detailed treatment of the interaction between radiative transfer and fog microphysics. J Atmos Sci 47 2153-2166.

Brown, R. and Roach, W.T. 1976 The physics of radiation fog: II - A numerical study. *Q J R Meteorol Soc*,102,335-354.

Brown, R. 1980 A numerical study of radiation fog with an explicit formulation of the microphysics. Q J R Meteorol Soc 106 781-802.

Cotton, W.R. and Anthes, R.A.,
1989 Storm and cloud dynamics. San Diego, Academic Press

Duynkerke, P.G. 1991 Radiation fog: a comparison of model simulation with detailed observations. Mon Wea Rev 119 324-341.

Eldridge, R.G. 1966 Haze and fog aerosol disributions, J.Atmos Sci 23, 605-613

Eldridge, R.G. 1971 The relationship between visibility and liquid water content in fog,, J.Atmos Sci 28, 1183-1186

Findlater, J., Roach, W.T. and McHugh, B.C.,
1989 The Haar of north-east Scotland. *Q J R Meteorol Soc*,115 581-608.

Golding, B.W. 1990 The Meteorological Office mesoscale Model, Metoerol Mag, 119,81-96.

Hanel, G. 1971 New results concerning the dependence of visibility on relative humidity and their significance in a model for

visibility forecast. Beitr. Phys. Atmosph. 44, 137-167.

Hanel, G. and Lehman, M. 1981 Equilibrium size of aerosol particles and relative humidity: New experimental data from various aerosol types and their treatment for cloud physics application. Contrib Atmos Phys54, 57-85.

Hanel, G. 1987 The role of aerosol properties during the condensational stage of cloud; A reinvestigation of numerics and microphysics, Beitr. Phys. Atmosph. 60, 321-339.

Hayden, C.M. and Purser, J.C. 1986 Applications of a recursive filter, objective analysis in the processing and presentation of VAS data, Preprint vol of 2nd Conference on satellite meteorology/remote sensing and applications, May 13-16, 1986, Williamsburg, Va. AMS, Boston Mass.

Hayden, C.M. and Purser, J.C. 1988 Three-dimensional recursive filter objective analysis of meteorological fields, Preprint vol of 8th Conference on Numerical Weather Prediction, Baltimore, Feb 1988.

Koschmeider, H. 1924 Theorie der horizontalen Sichtweite, Beitr. Phys. Atmosph, 12:33-53; 171-181.

Kunkel, B.A. 1983 Parameterization of droplet terminal velocity and extinction coefficient in fog models, J. Clim. and Appl. Meteor., 23, 34-41

Meyer, M.B., Jiusto, J.E. and Lala, G.G.
1980 Measurements of visual range and radiation-fog(haze) microphysics, J Atmos Phys 37, 622-629

Middleton, W.E.K. 1952 Vision through the atmosphere, Toronto, University of Toronto Press.

Musson-Genon, L., 1987 Numerical simulation of a fog event with a one- dimensional boundary layer model. *Mon Wea Rev*,115,592-607.

Oliver, D.A., Lewellen, W.S. and Williamson, G.G.
1978 The interaction between turbulent and radiative transport in the development

of fog and low-level stratus. J Atmos Sci 35 301-316.

Pilie, R.J., Mack, E.J., Rogers, C.W., Katz, U. and Kocmond, W.C. 1979 The formation of marine fog and the development of fog-stratus along the California Coast. *J Appl Meteorol*,18,1275-1286.

Pinnick, R.G., Hoihjelle, D.L., Fernandez, G., Stenmark, E.B., Lindberg, J.D., Hoidale, G.B. and Jennings, S.G. 1978 Vertical structure in atmospheric fog and haze and its effect on visible and infrared extinction., J.Atmos Sci, 35, 2020-2032

Purser, J.C. and McQuigg, R. 1982 A successive correction analysis scheme using recursive numerical filters, Met O 11 Tech Note No 154, available from National Met library, Meteorological Office, London Road , Bracknell, England

Roach, W.T., Brown, R., Caughey, S.J., Garland, J.A., and Readings, C.J. 1976 The physics of radiation fog I - a field study. Q J R Meteorol Soc 102 313-333

Tjernstrom, M. 1987 A study of flow over complex terrain using a three dimensional model. A preliminary model evaluation focussing on stratus and fog. Annales Geophysicae 5B 469-486.

Tomasi, C. and Tampieri, F. 1976 Features of the proportionality coefficient in the relationship between visibility and liquid water content in haze and fog. Atmosphere, 14, 61-76.

Tremant, M., 1989 The forecasting of sea fog. *Meteorol Mag*,118,69-75.

Turton, J.D. and Brown, R. 1987 A comparison of a numerical model of radiation fog with detailed observations. Q J R Meteorol Soc 113 37-54.

Vehil, R., Monerris, J., Guedalia, D. and Sarthou, P. 1989 Study of radiative effects (long-wave and Short-wave) within a fog layer. Atmos Res 23 179-194.

Wright, B.J. and Golding, B.W. 1990 The Interactive Mesoscale Initialisation, Meteorol Mag, 199,234-244.

Zdunkowski,W.G. and Barr, A.E.
1972 A Radiative-conductive model for the prediction of radiation fog Boundary-layer Met 3 152-177.

APPENDIX A - Symbols and Abbreviations Used

A^0	Curvature parameter
B^0	Activation parameter
B	Luminance of background
B'	Luminance of object
B_b	Luminance of black object
B_h	Luminance of the horizon sky
C	Contrast
C_0	Contrast of object and horizon sky when both are seen at close range
C_R	Contrast of object and horizon sky when both are seen at a distance R
CCN	Cloud condensation nuclei concentration (cm^{-3})
CWMR	Cloud water mixing ratio ($KgKg^{-1}$)
CMWR'	Cloud water mixing ratio deduced from visibility analysis ($KgKg^{-1}$)
CW'	'Subgridscale' cloud water mixing ratio ($KgKg^{-1}$)
CW	Gridscale or subgridscale cloud water mixing ratio, whichever is larger ($KgKg^{-1}$)
Q_{ext}	Normalised extinction cross-section
r	Distance / Volume equivalent radius of particle (m)
r_d	Volume equivalent radius of dry particle (m)
R	Distance
RH	Relative humidity (fraction)
RH^{low}	Lower limit of relative humidity in lowest 20m (fraction)
RH^{high}	Upper limit of relative humidity in lowest 20m (fraction)
vis	Visibility (km)
W	Liquid water content (gm^{-3})
β	Extinction coefficient (fraction)
ε	Threshold contrast
ρ_a	Density of air (Kgm^{-3})
ρ_w	Density of water (Kgm^{-3})

APPENDIX B

The use of the analysis scheme in the IMI

A subroutine 'ANALYS' is called a number of times in the IMI to provide the required analyses of several variables in the model using the recursive filter analysis scheme. The routine performs two main steps. Firstly, data from the observation points are used to modify the first-guess field, and secondly, the modified field is smoothed (using the subroutine 'SMEAR'). In some cases, the observations themselves are used in the modification, while in others, either the logarithm of the observations, or the difference between the observations and the background field is used.

Various parameters used by 'ANALYS' are set initially by calling a subroutine 'ANAL1'; these may vary depending on which variable is being analysed. For example, some analyses include the edge points while others exclude them; different analyses use different sets of values for the 'tolerance' assigned to observations. The tables below summarise those

variables which are actually analysed. In each case, the parameters used are also shown.

Variables which are analysed

Variable	IANL	ILOG	IEDGE	RMIN	RMAX	RF	TOLMIN	TOLMAX	TOLINC
Visibility	var	log	inc	0	4	0.5	10^6	10^6	0.7
Pressure	diff	var	inc	1	7	0.8	0.1	4.0	0.5
Temperature	diff	var	inc	1	7	0.8	1.0	5.0	0.5
Cloud cover	var	var	inc	0	4	0.5	8.0	8.0	0.7
Cloud base height	var	log	inc	0	4	0.5	10^6	10^6	0.7
Dew point	diff	var	inc	1	7	0.8	1.0	5.0	0.5
Precipitation rate	var	var	inc	0	4	0.5	10^6	10^6	0.7
Accumulated pptn.	var	log[1]	inc	0	2	0.5	2.0	4.0	0.7
U component of wind[2]	diff	var	exc	1	7	0.8	2.0	10.0	0.6
V component of wind[2]	diff	var	exc	1	7	0.8	2.0	10.0	0.6

where

IANL=1 (diff) - analyse difference between observation and background field
=2 (var) - analyse variable itself
ILOG=1 (log) - analyse logarithm of variable
=0 (var) - analyse variable itself
IEDGE=0 (inc) - include edge points
=1 (exc) - exclude edge points
RMIN, RMAX - minimum and maximum radii of smoothing in gridlengths
RF - 'pointedness' of Gaussian
TOLMIN,TOLMAX - minimum and maximum tolerance values over several scans
TOLINC - measure of change of tolerance between scans

Other variables are set in 'ANAL1' along with those listed above, and then left unchanged. These are:

NSCAN=3 - number of scans over grid
NSMOO=2 - number of smoothing sweeps within each scan
RINC=0.5 - (supposedly) measure of change of radius of smoothing between scans. (Not used at present)

Notes

1. In actual fact, the variable which is analysed is log(2-ap), where ap=accumulated precipitation. This is to allow for large negative values of the variable (representing lying snow). Taking logarithms prevents excessive spreading of depths of snow.

2. The U and V components of the background field wind are actually offset by half a grid length in the X and Y directions respectively.

OPERATIONAL MESOSCALE
FORECAST DATA TIME 0Z 14/12/91

FIGURE 1

PREDICTED VISIBILITY
AND PRECIPITATION

F = VISIBILITY < 1KM
– = VISIBILITY 1–5KM

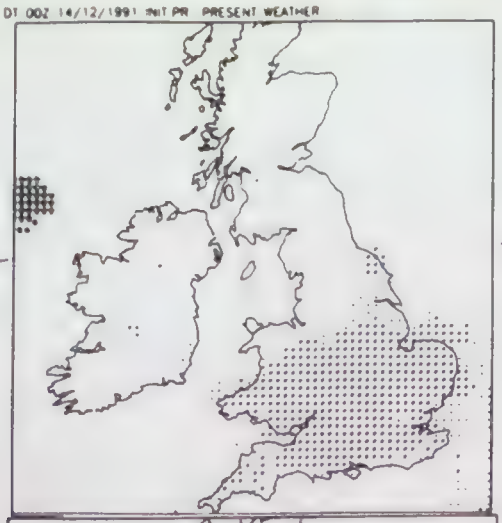

0UTC T+0

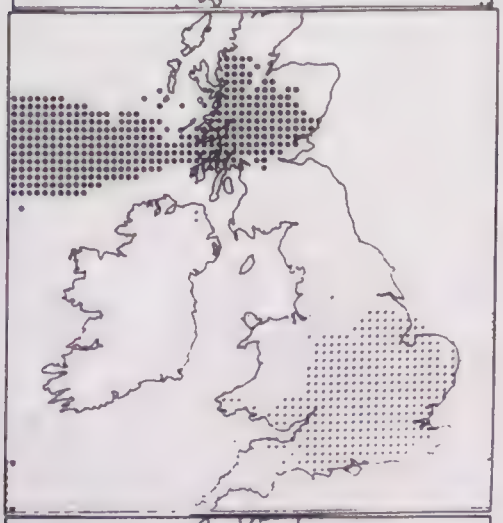

6UTC T+6

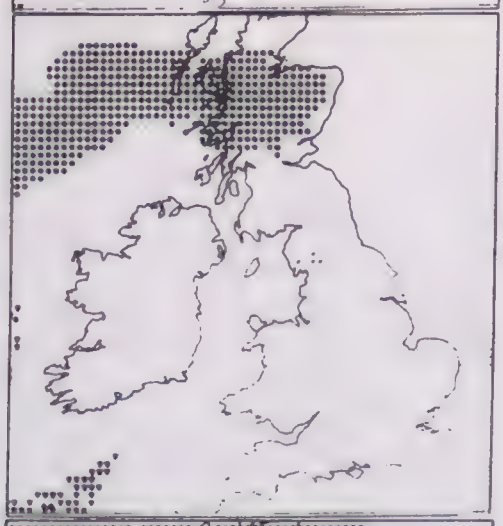

12UTC T+12

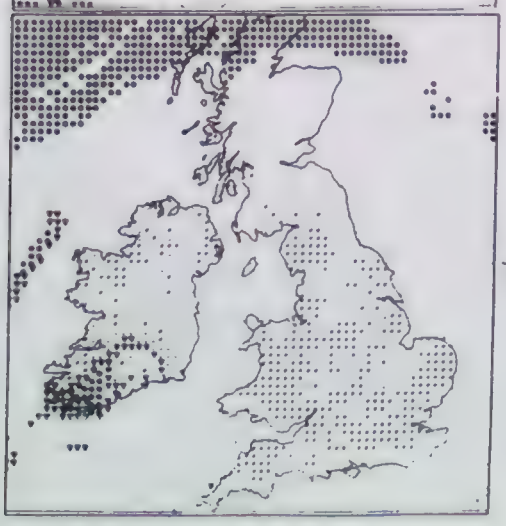

18UTC T+18

OPERATIONAL MESOSCALE
FORECAST DATA TIME 6Z 14/12/91

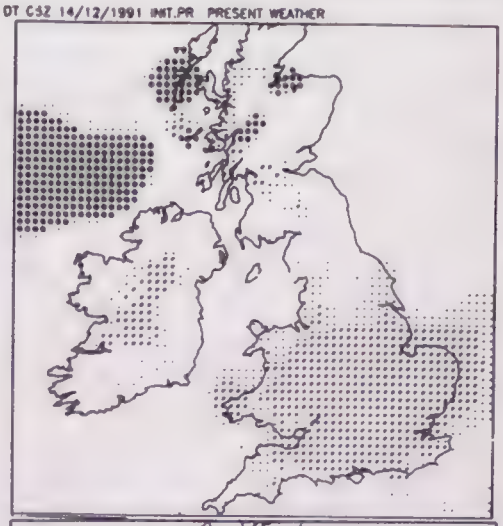

T+0

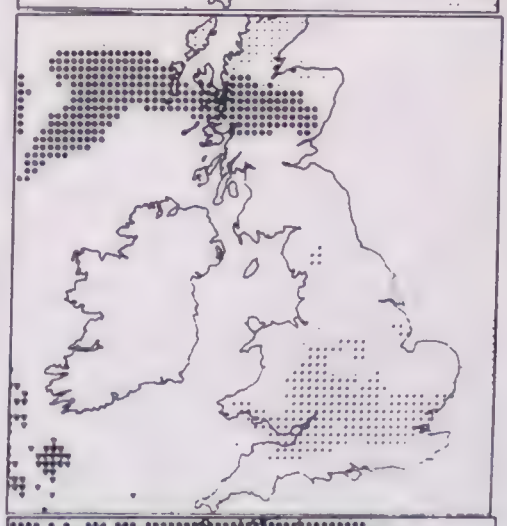

T+6

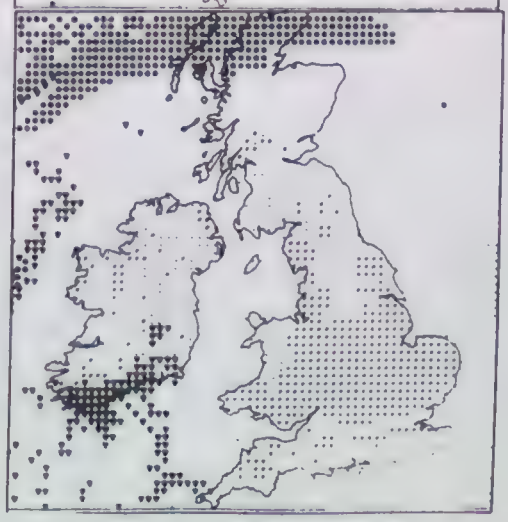

T+12

OPERATIONAL MESOSCALE FORECASTS

DATA TIME 6Z 14/12/91 DATA TIME 0Z 15/12/91

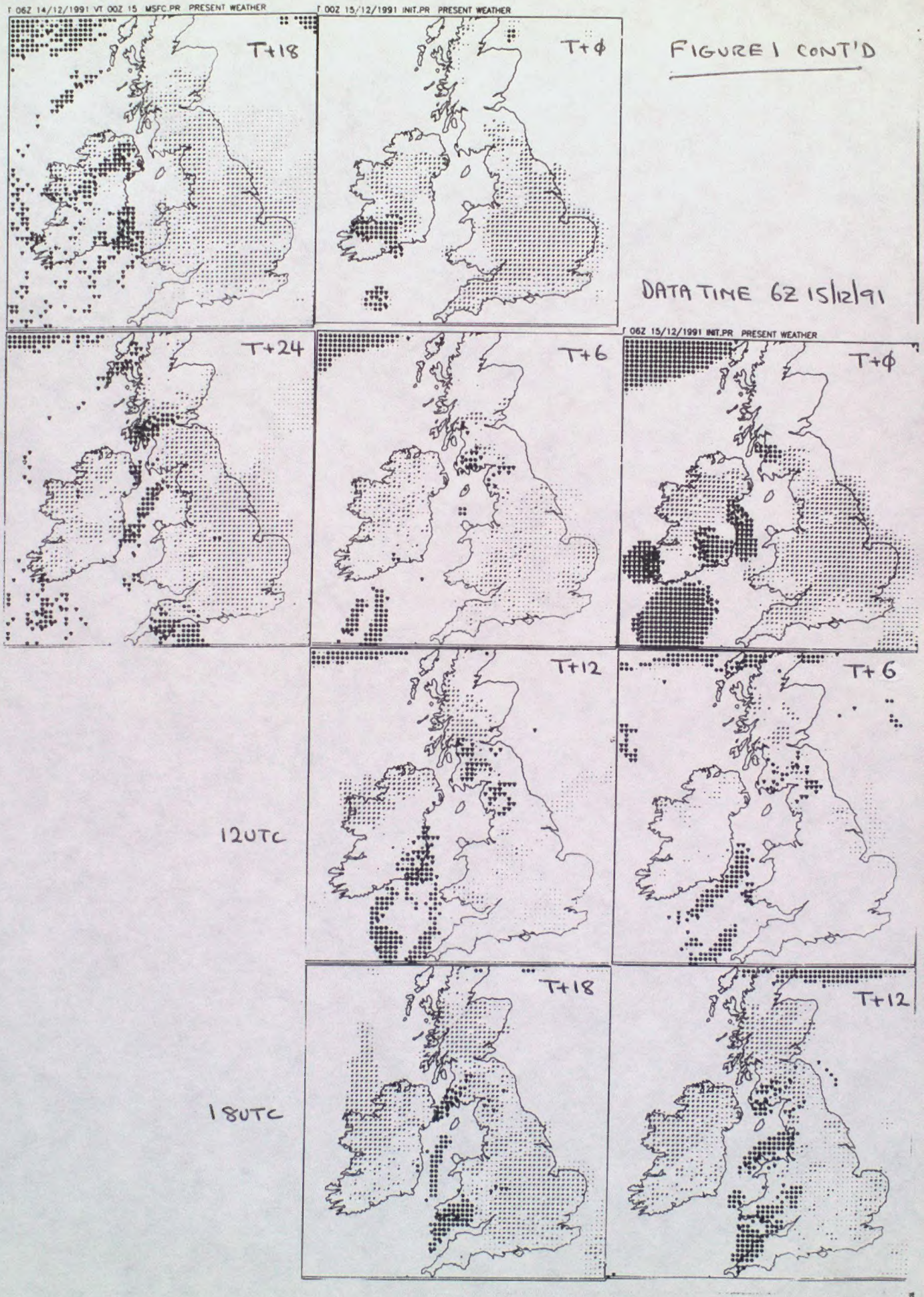

FIGURE 1 CONT'D

FIGURE 2

COMPARISON OF OBSERVED VISIBILITY WITH PREDICTED VISIBILITIES FROM HIGH RESOLUTION UNIFIED MODEL AND CURRENT MESOSCALE MODEL WITHOUT VISIBILITY ANALYSIS - FORECASTS FROM DATA TIME 6UTC 14th DECEMBER 1991

F < 200m , F 200m - 1km , - 1-5 km

HIGH RESOLUTION UNIFIED MODEL

MESOSCALE FORECAST FROM INTERPOLATED REGIONAL MODEL FIELDS

OBSERVATIONS

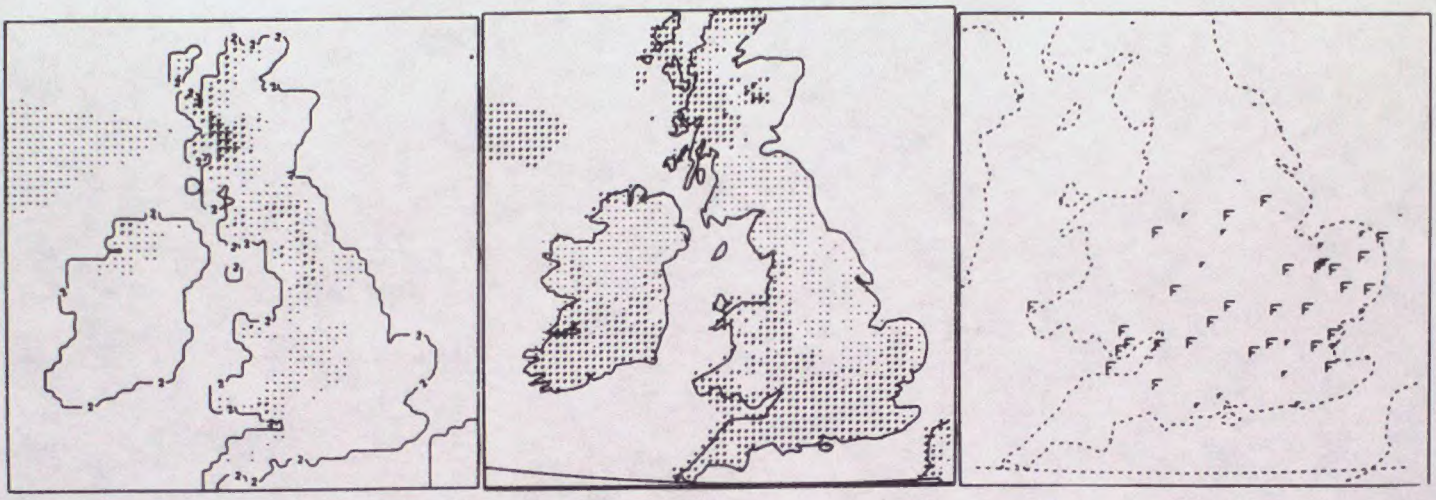

T+0 valid 6UTC

T+0 valid 6UTC

6UTC

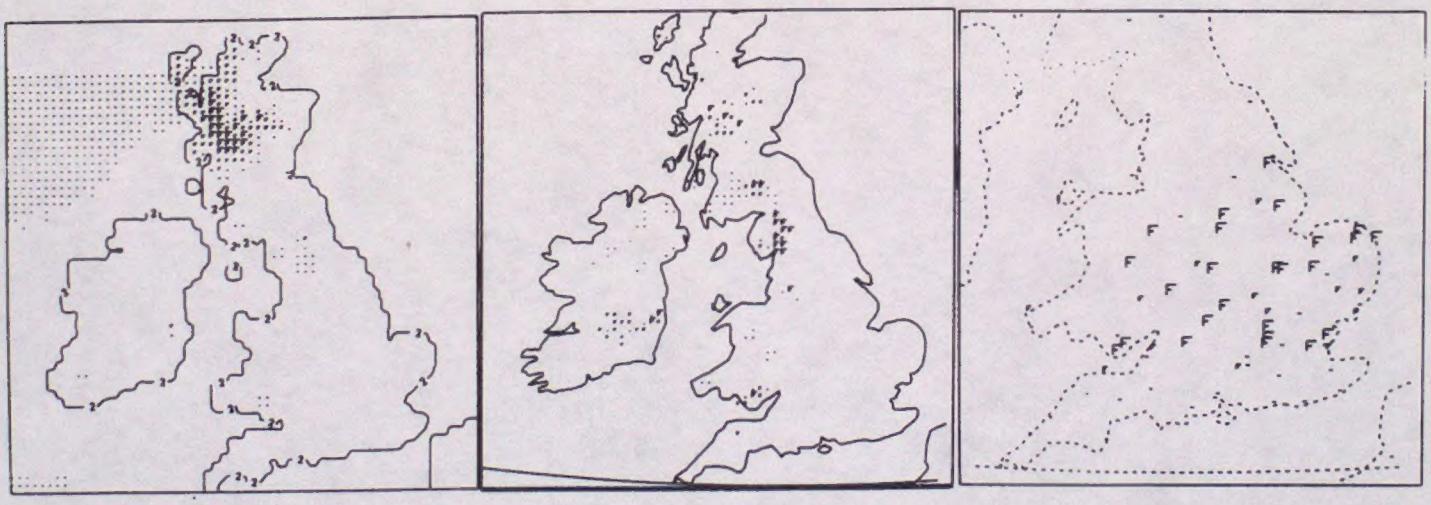

T+6 valid 12UTC

T+6 valid 12UTC

12UTC

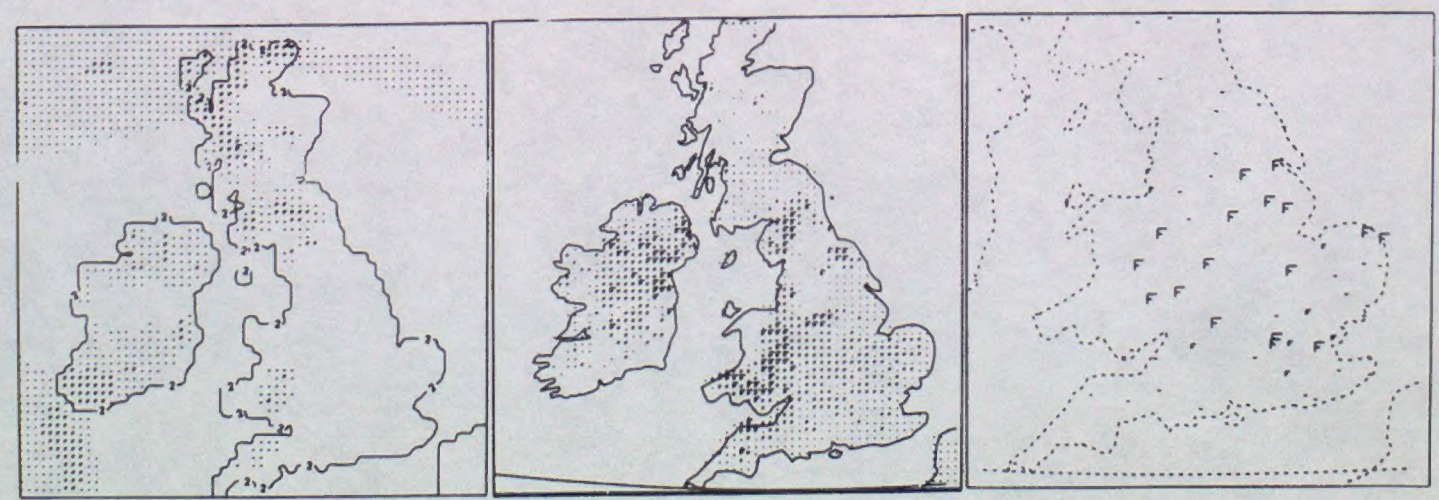

T+12 valid 18UTC

T+12 valid 18UTC

18UTC

FIGURE 2 continued

COMPARISON OF OBSERVED VISIBILITY WITH PREDICTED VISIBILITIES FROM HIGH RESOLUTION UNIFIED MODEL AND CURRENT MESOSCALE MODEL WITHOUT VISIBILITY ANALYSIS - FORECASTS FROM DATA TIME 6UTC 14th DECEMBER 1991

F < 200m , F 200m - 1km , - 1-5 km

HIGH RESOLUTION UNIFIED MODEL	MESOSCALE FORECAST FROM INTERPOLATED REGIONAL MODEL FIELDS	OBSERVATIONS

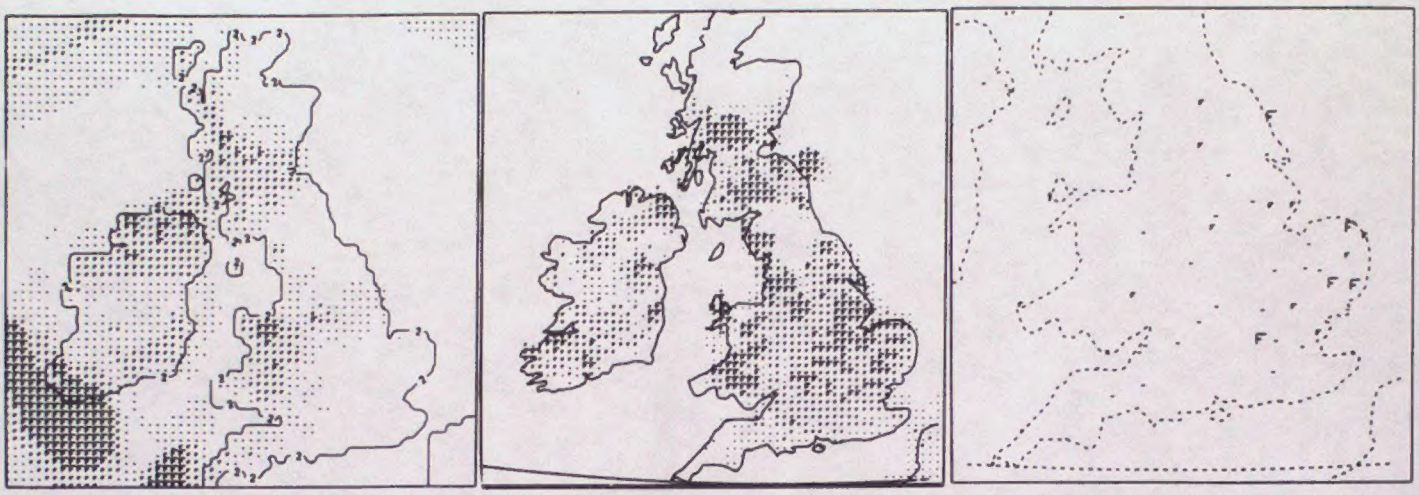

T+18 valid 0UTC 15 Dec | T+18 valid 0UTC 15 Dec | 0UTC 15 Dec

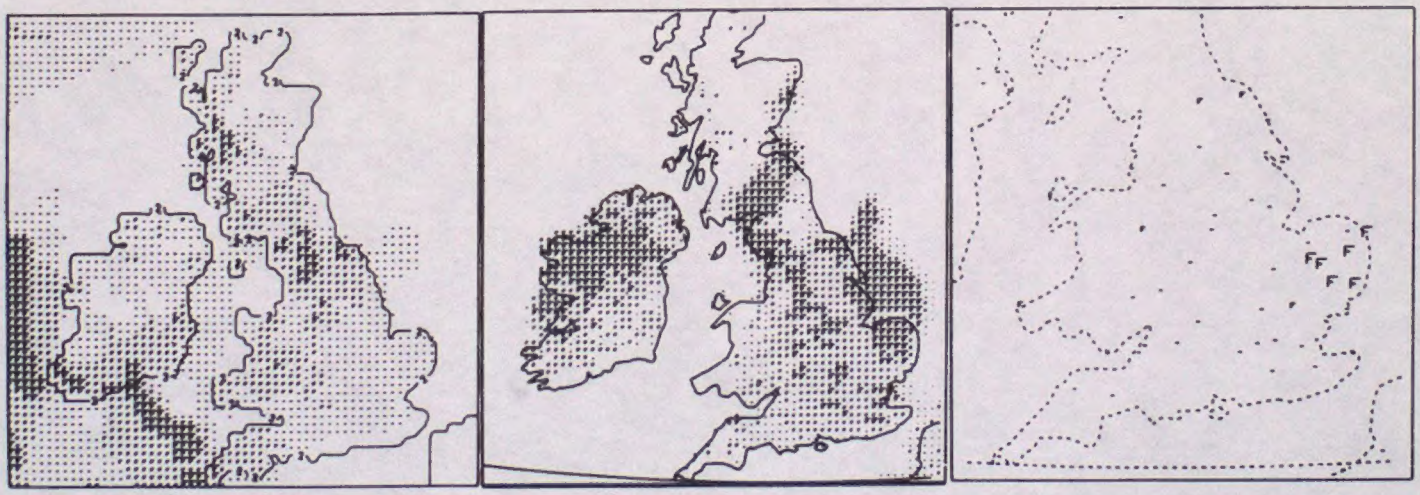

T+24 valid 6UTC 15 Dec | T+24 valid 6UTC 15 Dec | 6UTC 15 Dec

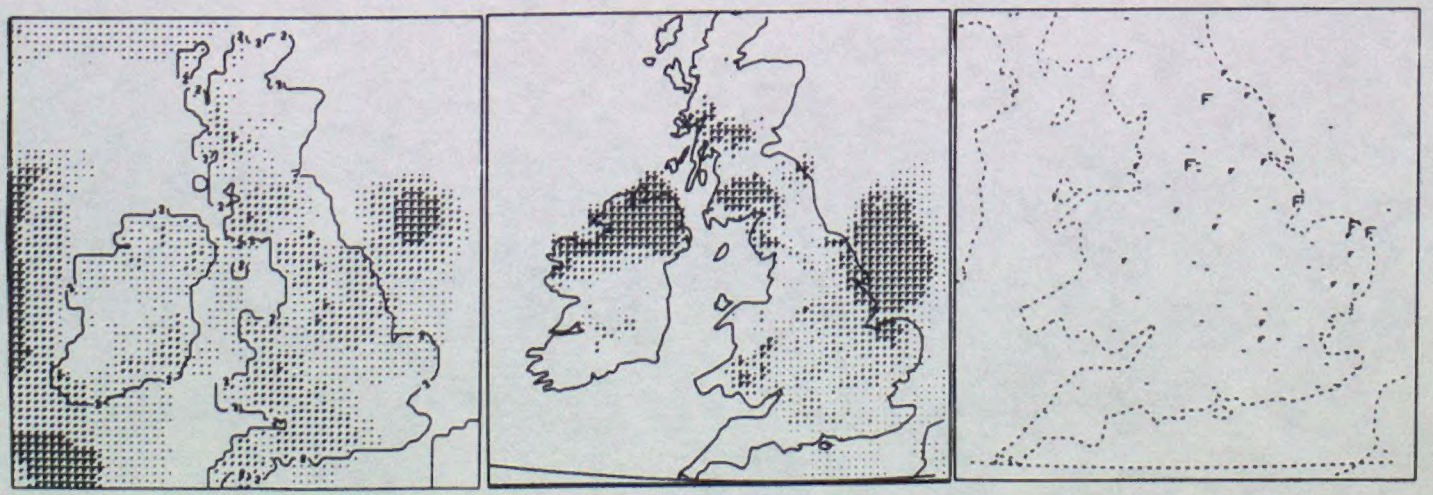

T+30 valid 12UTC 15 Dec | T+30 valid 12UTC 15 Dec | 12UTC 15 Dec

SHORT RANGE FORECASTING DIVISION SCIENTIFIC PAPERS

This is a new series to be known as Short Range Forecasting Division Scientific Papers . These will be papers from all three sections of the Short Range Forecasting Research Division i.e. Data Assimilation Research (DA),Numerical Modelling Research (NM), and Observations and Satellite Applications (OB) the latter being formerly known as Nowcasting (NS). This series succeeds the series of Short Range Forecasting Research /Met O 11 Scientific Notes.

1. **THE UNIFIED FORECAST /CLIMATE MODEL .**
   M.J.P. Cullen
   September 1991

2. **Preparation for the use of Doppler wind lidar information in meteorological data assimilation systems**
   A.C. Lorenc, R.J. Graham, I. Dharssi, B. Macpherson, N.B. Ingleby, R.W. Lunnon
   February 1992

3. **Current developments in very short range weather forecasting.**
   B.J. Conway
   March 1992

4. **DIAGNOSIS OF VISIBILITY IN THE UK MET OFFICE MESOSCALE MODEL AND THE USE OF A VISIBILITY ANALYSIS TO CONSTRAIN INITIAL CONDITIONS**
   S.P. Ballard, B.J. Wright, B.W. Golding
   April 1992